

# Offshore Wind Farm Export Cable Current Rating Optimisation

James Pilgrim<sup>1</sup>, Simon Catmull<sup>2</sup>, Richard Chippendale<sup>1</sup>, Richard Tyreman<sup>3</sup> and Paul Lewin<sup>1</sup>

1. Tony Davies High Voltage Laboratory, Southampton University, jp2@ecs.soton.ac.uk

2. RES Offshore, Kings Langley, Simon.Catmull@res-offshore.com

3. Centrica Renewable Energy Ltd, Windsor

**Abstract:** The appropriate sizing of subsea export systems for offshore wind farms presents a number of challenges when striking an appropriate balance between design conservatism and cost effectiveness. Several areas of potential conservatism have been investigated through numerical modelling that has been backed by data that has been obtained from experimental 132kV 3-phase submarine cable.

**Keywords:** Cable, HVAC, Armour Loss, J-Tube, Modelling.

## 1 INTRODUCTION

Export cables represent an area of significant capital expenditure in the construction of an offshore wind farm. In order to bring down the cost of energy associated with offshore wind and maintain its viability as a form of renewable generation, the design of wind farm export systems needs to be efficient. In the case of export systems, this requires that the subsea cables transmitting the power to shore have sufficient current carrying capacity (or ampacity) that the conductor temperature will not exceed its permissible threshold. This paper seeks to present an overview of work done to identify areas of conservatism within the standard current rating approach, and to quantify the impact that they have on the current rating of the cable.

The IEC60287 standard calculation method [1] is the means by which an Engineer would normally ensure that the conductor temperature remains within the threshold of the insulating material. IEC60287 makes use of a thermal network approach to represent the heat generation and dissipation in a cable. It is simple to use but contains inherent assumptions and simplifications. Its primary purpose is to provide a steady state rating which ensures that the conductor temperature does not exceed that at which the insulating material

will begin to degrade. Sub-sea cables commonly use cross-linked polyethylene (XLPE) as the insulating material, which typically has a thermal limit of 90°C. There are two main sources of heat generation, also known losses, within a power cable [2]. These are current dependant losses and voltage dependant losses. Current dependant losses are those generated within conductive components of a cable. For a subsea cable these will typically consist of the conductors, sheaths and armouring. Voltage dependant losses result from losses within the dielectric. Work done by a cable manufacturer suggests that the representation of armour losses in the design standard is conservative [3]. Additional areas of conservatism common in the rating of wind farm cables are the assumptions of uniform burial and constant load. As a subsea cable makes landfall it is liable to experience burial of varying and complex nature. Overly simplifying the thermal representation of this burial can lead to an inaccurate estimation of the ampacity of the cable. A wind farm is an inherently variable form of generation, which has a power output that it is broadly predictable over the long term but less so in the short term. As a result it is assumed that the cable experiences a continuous and full output from the wind farm when determining the rating. This approach does not take into consideration that the power output of wind farms is inherently linked to a dynamically varying set of weather conditions, meaning that it is rare to achieve long periods of full rated power output. Thus the application of continuous ratings, which assume constant power transfer in the export cable for the life of the cable, is likely to lead to some conservatism in the sizing of the cable system.

In order to determine the potential level of conservatism associated with these assumptions, Centrica Renewable Energy Ltd commissioned a program of research at

the Tony Davies High Voltage Laboratory at Southampton University that consisted of components of experimental and modelling works. This paper presents an overview of the work undertaken and the potential impact that the findings would have upon the rating.

## 2 METHOD

The factors affecting the rating of a cable that this work sought to better understand were:

- Current dependant losses in the cable, specifically those associated with the armouring.
- Time dependant nature of conductor temperature.
- Impact of a more detailed representation of complex burial environments.

This was achieved through a combination of experimentation and numerical modelling. In summary, a length of 3-core, 132kV subsea cable had a number of load current profiles applied while the temperature and current data obtained from conductive components of the cable were recorded. This data was used as a means of refining and validating finite element models (FEM) of the cable. The validated cable FEM was implemented within larger models representing potentially thermally limiting locations along an export route, namely the landfall and within a J-Tube.

### 2.1 EXPERIMENTAL TESTING

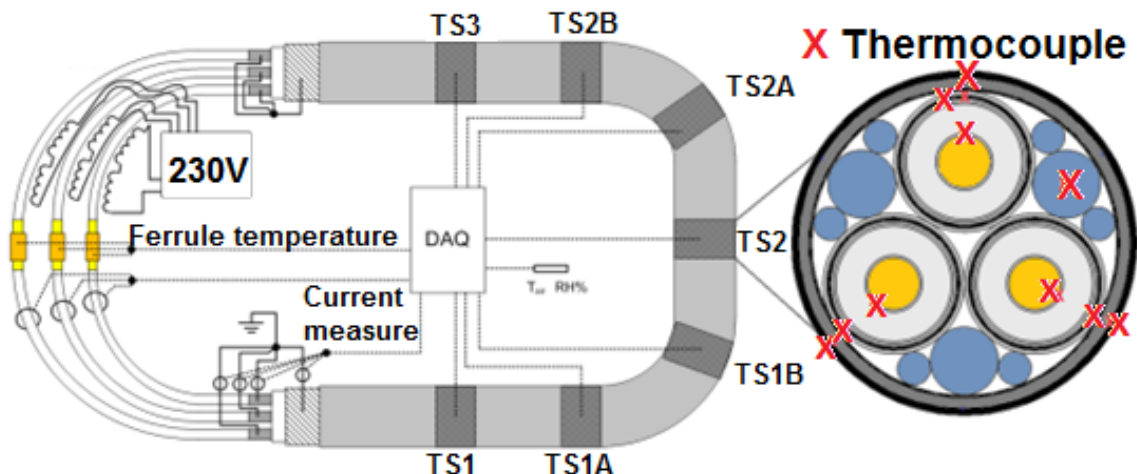
In order to ensure that the results of the overall study were as representative as possible of a real system, it was desirable to acquire experimental data to demonstrate

the thermal performance of the cable system. In order to reproduce the same thermal behaviour as that seen in the field, it was not necessary to conduct experimental tests at rated voltage (although it should be noted that a small, voltage dependent dielectric loss exists which is accounted for in the final models). This means that the circuit could be energized with load current only. The outputs of the experiments were as follows:

- Measurements of load current over time.
- Measurements of induced currents over time.
- Temperature profiles for metallic components (conductor, sheath, armour wires).
- Temperature profile of ambient environment.
- Distributed Temperature Sensor data from the fibre optic sensor, along with additional point thermocouple measurements along the length

These outputs were obtained for a number of stepped load profiles that were applied to a 3-phase subsea cable with conductor core cross sectional area (CSA) of  $630\text{mm}^2$ , a rated voltage of 132kV and the cable either in air or submerged in water. The experimental setup used is shown in Figure 1. Currents of up to 1000A were induced in each core using 2 current transformers in series, per phase. The sheaths and armouring were star pointed at both ends of the cable with one end being earth bonded. Current was measured at 10minute intervals in each of the cores and the earth bonds for the sheath and armouring. Temperature was measured throughout the length of the cable using an Oryx Distributed Temperature Sensor (DTS) unit provided by Sensornet and at the Test Sites (TS)

Figure 1



indicated in Figure 1 using K-type thermocouples. The thermocouples were placed in contact with each of the conductor cores, their respective sheaths and within the armouring. Ensuring that the thermocouples were in good contact with the desired component was critical element of the measurement process. It was desired that the thermocouples be installed in the most non-intrusive way possible, meaning that it was not feasible to obtain visual confirmation that the thermocouples were sited correctly. Although an invasive method would provide greater certainty that each thermocouple was precisely located, it was considered likely that the experimental results would be adversely impacted. Hence a trade-off existed between visual confirmation and measurement accuracy. To minimise the risk of an incorrectly placed thermocouple, the following process was used:

1. Thermocouples were only sited at metallic components (conductor, lead sheath, steel armour and the metallic covering of the fibre optic tube).
2. All metallic components of the cable were electrically connected to a common rail.
3. The common rail was connected through a continuity meter to a hand drill.
4. An audible signal would be given when the drill bit struck a metallic component.
5. By sequentially removing the link between each component and the common rail, it was possible to identify which metallic component had been struck.
6. The drill bit could then be retracted and a thermocouple inserted, with the thermocouple then connected to the continuity meter to verify its location.
7. Once good continuity had been obtained between the thermocouple and the component, nylon filament was then used to secure the thermocouple into place.

This system was found to be very efficient at placing thermocouples accurately, although the process is time consuming. Some problems were experienced in terms of “false positive” readings, as the impedance between the sheath and armour is low by design.

With the test length of cable suitably instrumented a series of load profiles were applied to the cable with it either in the air or

submerged in freshwater. The figures below are an example of the data obtained when a step load of approximately 1000A was applied to a dry cable for a period of 40 hours. Figure 2 shows the current profile in the cable cores and it can be seen that there is small current imbalance between the phases, with phase 2 approximately 5% greater than phase 3. This was considered to be small enough to be negligible, as it could be directly accounted for in the finite element models.

Figure 2

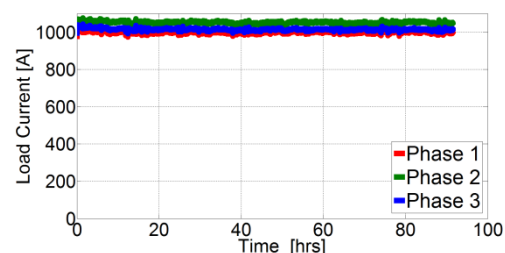


Figure 3 shows the variation in sheath and armour currents with time and it can be seen that there is a noticeable trend in the sheath currents as the temperature of the sheath rises, with a reduction in current of around 10% as a result of the change in sheath resistance.

Figure 3

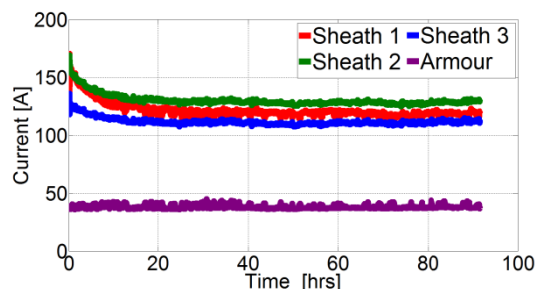
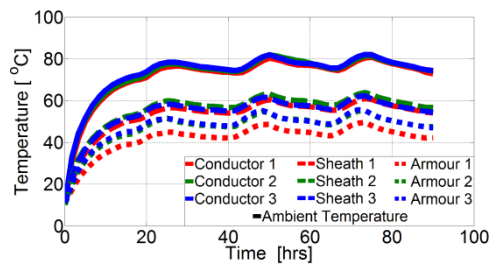


Figure 4 shows the variation in temperature of conductive elements within cable. The figure demonstrates a clear temperature profile extending radially out from the conductor core.

Figure 4



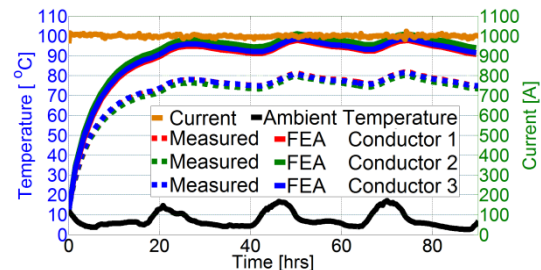
## 2.2 CABLE MODEL DEVELOPMENT

The data obtained through experimentation were used as a benchmark against which the performance of the finite element model could be tested. The starting point was a model which replicated the IEC 60287 approach (including use of standard values for electrical/thermal parameters), before moving to identify areas which seem to cause the model results to deviate from the measured values.

The data presented in this section is based on a model of the cable system developed to be identical to the manufacturers drawing, using the same thermal and electrical parameters as the IEC 60287 analysis. This is a transient model, complete with input of the measured ambient air temperatures and load current as per the experiments. The electrical resistances are calculated using the standard IEC equations, but with the benefit of temperature correction. Joule losses are based on the recorded conductor currents, with the sheath losses being assumed to be entirely due to circulating currents. As the armour losses are primarily magnetic losses (not from circulating current), they are initially modelled using the IEC 60287 equation. The modelled geometry of the filler material in the interstices is based upon the drawing. Thermally, it is assumed that heat can be transferred by conduction, or by radiation between individual black body surfaces (for instance from the filler to the armour bedding), but that convection transfer within the interstices cannot occur. This assumption is sensible based upon the restricted size of the air gaps between the fillers. Heat transfer from the surface of the cable is achieved through both convection and radiation. Shown in Figure 5 is a comparison between the conductor temperature obtained from model predictions and the measured data from a

stepped load applied to the test length in water. From this figure it is apparent that the initial finite element model considerably overestimates the cable conductor temperatures in steady state.

Figure 5



In Figure 6 and Figure 7 it can be seen that the temperature differential between the sheath and armour is also considerably higher than that measured, suggesting that the heat transfer within the interstices is better in reality than the model assumes.

Figure 6

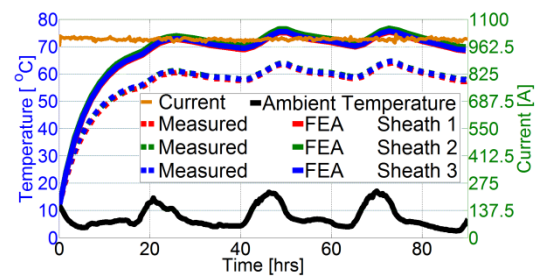
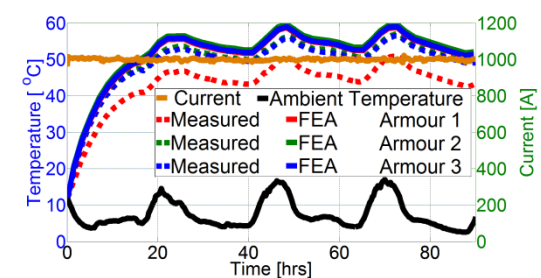


Figure 7



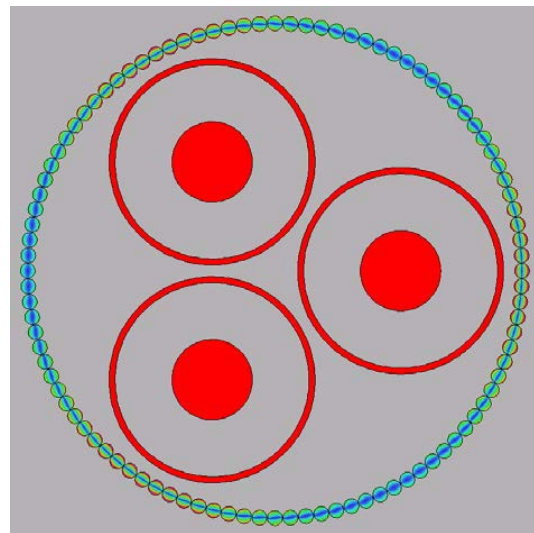
While the modelled armour temperature generally provided a reasonable match to the experimental data, the modelled sheath temperature was considerably higher than the experimental values would suggest – thus suggesting that the thermal resistance between the two was excessively high.

Physical inspection of the test cable showed that the visible volume of air in the interstices was small. Radiation heat transfer is generally less efficient than conduction transfer, leading to the assumption that the model approach was underestimating the conduction transfer. Analysis of the experimental data suggested that the thermal resistance between the sheath and armour could be well approximated by assuming that the entire region was filled with polypropylene. Making this assumption immediately brought the sheath temperatures into closer agreement. Given that a physical basis could be observed for making this assumption, the interstices were modelled as a solid region whose thermal conductivity was estimated using the mixture rule according to the volumetric proportion of air and polymer which should have been present according to the manufacturer's drawings.

Having examined the properties of the filler, the conductor temperatures predicted by the model were still in excess of that seen from the experiment. Two possible causes existed, namely that the model was overestimating conductor losses (high AC resistance) or that the model was overestimating the thermal resistivity between the conductor and sheath. As the measured DC resistances agreed well with the calculated values, this was considered unlikely. It is common practice to assume that the thermal conductivity of semi-conducting screen layers matches that of the insulation itself. However, the two materials are different, despite using the same base polymer. The polyethylene used in the conductor and insulation screens is generally heavily filled with carbon black (or similar materials) in order to make the insulating base polymer somewhat more conductive (a requirement for it to act as a stress relieving layer). Given the large increase in electrical conductivity (the bulk resistance of the semi-conductive layer over the lead sheath, for example, was measured to be only 140Ω), it seemed logical that an increase in thermal conductivity would also result. Based on analysis of the experimental data, the thermal conductivity of the screen layers was increased from  $0.3\text{Wm}^{-1}\text{K}^{-1}$  to  $0.5\text{Wm}^{-1}\text{K}^{-1}$ . This provided a better match to the experimental data, and was considered to be a justifiable assumption.

The magnitude of armour losses for 3 phase submarine cables has been widely discussed in the cable community, with publications by some manufacturers claiming to demonstrate that the IEC 60287 equations lead to higher losses than are physically observed [3]. Although no general guidelines have yet been found, the standard equation is widely considered to provide conservative results. After making the above changes to the filler and screen parameters, it was noted that in some results the armour temperatures were still slightly higher than measured. It was found that reducing the armour loss by 40% (in broad agreement with the results presented in [3]), a better agreement between the modelled and measured temperatures was obtained. To deliver further rigour to this

Figure 8



analysis, a bespoke electromagnetic model was constructed with the intention of providing greater validation of the eddy current/magnetic losses within the armour.

Detailed discussion of the results obtained from the electromagnetic model is beyond the scope of this article but in summary, two different 2D modelling options were initially compared against IEC60287. First a simple 2D slice model was created with all armour wires modelled explicitly, shown in 8. Secondly the armour was represented as a single annular region with equivalent thickness and material properties, as shown in Figure 9



Figure 9

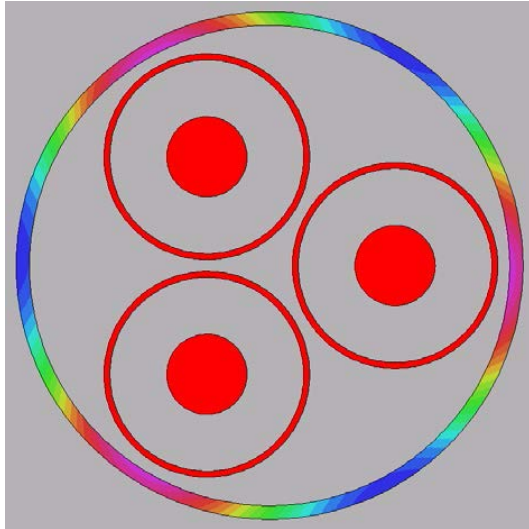


Table 1, below, summarises the results obtained from the 2 models when compared to an IEC representation of the losses. In addition the results for a model without steel armour wires are presented as an aid to explaining the phenomena seen.

All results in Table 1 have been obtained for a balanced load of 1000A on a 132kV cable with conductor cross-section of 630mm<sup>2</sup>. A number of important points can be drawn from Table 1. Considering first the model without armour, we note that the circulating current and eddy currents are both considerably lower than the models where armour is modelled. This is due to the effect of the permeable armour layer enabling the phase currents to drive more flux around and through the screens, thus leading to bigger circulating currents and eddy currents. The plain 2D model is not able to fully represent the hysteresis losses within the armour wires, hence explaining the very

Table 1

Parameter	No Armour / Non Conductive Armour	Plain 2D Model	Equivalent Material	IEC 60287 data at 20°C
Sheath Circulating Current Losses (W/m per core)	6.6	8.3	9.8	9.8
Sheath Eddy Current Losses (W/m per core)	1.9	2.5	3.1	0
Total Sheath Losses (W/m per core)	8.5	10.9	12.9	9.8
Armour Losses (W/m)	0	0.3	7.4	42.5

low magnitude of armour losses in this case. The armour losses from the equivalent material model are observed to be much greater, at approximately 7.5W/mK for the balanced condition. Considering the IEC 60287 armour loss term, it is apparent that the electromagnetic FEM show a much lower magnitude of armour loss than the IEC model predicts.

Having examined the sources of the discrepancies between the initial model and the experimental data, along with carrying out a comprehensive programme of electromagnetic modelling to reduce the uncertainty around induced losses, FEA results were again compared to the experimental data. The results of comparing the final benchmarked cable model against the experimental data for a step load of 1000A for 40 hours are shown in the following figures. The modelled conductor temperatures shown in Figure 10 closely match the measured ones during the initial heating stage, ending with the model predicting temperatures of 10°C above those measured in the experiment.

Figure 10

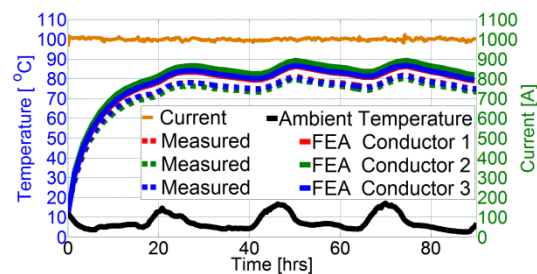


Figure 11

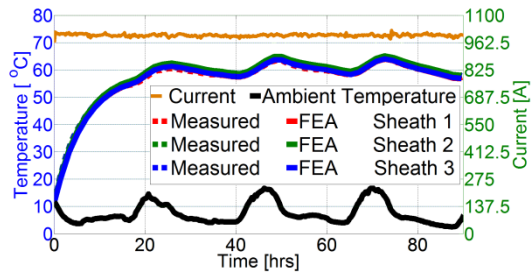
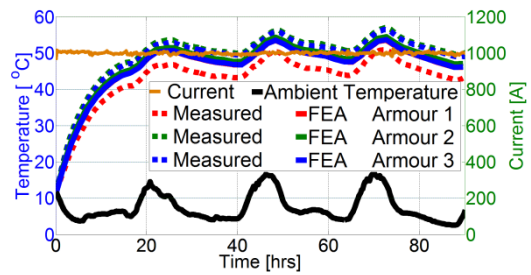


Figure 11 shows the comparison of modelled and measured sheath temperatures. The match to the experimental data is extremely good with the modelled data sitting in the middle of the measured experimental range. Likewise, Figure 12 shows the armour temperature comparison, with the results sitting directly in the middle of the experimental data ranges.

Figure 12



Based on the data presented within this section, we believe that the model developed provides an adequate prediction of cable temperatures to be carried forward for rating calculations. It is clear that some conservatism remains regarding conductor temperature prediction, however we believe that this is appropriate given the need to guard against the effect of uncertainties.

### 2.3 MODELLING

Having developed a cable FEM that was well validated against experimental data it was subsequently used to better understand the performance of a cable in thermally challenging locations and what the key sensitivities are. The locations investigated are a landfall and within a J-Tube

### 2.4 LAND FALL

Cable land falls present a number of challenges to the rating of a subsea cable. This can be the result of rapidly varying burial depth and the burial material thermal properties varying with depth. Figure 13 shows the cable (denoted by the red dashed

line) burial of varying depth and soil thermal resistivity, where the resistivity values are given in Table 2.

Figure 13

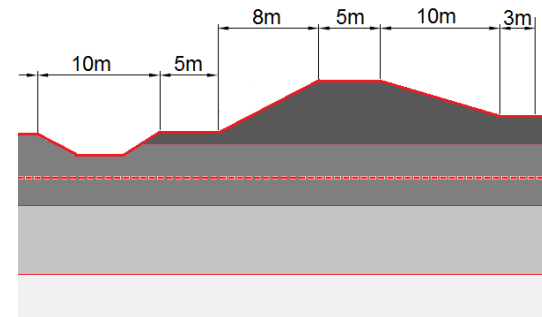


Table 2

Depth Range	Thermal Resistivity
0-5m	1.20KmW <sup>-1</sup>
5-10m	0.71 KmW <sup>-1</sup>
10-25m	0.56 KmW <sup>-1</sup>
>25m	0.58 KmW <sup>-1</sup>

Due to the 1D representation of the buried cable assumed by IEC 60287, it is necessary to assume that the burial depth was constant along the length of the cable and that depth would be equivalent to the deepest point. In addition, an assumption would need to be made that the thermal resistivity would be consistent throughout the burial. To demonstrate the variation in rating that could be achieved for a cable of CSA = 630mm<sup>2</sup> and rated voltage of 132kV, a rating based on the design standard is compared against a 2D FEM with IEC losses and a 2D FEM with benchmarked losses obtained through the previously described experimentation. The ratings were obtained for a burial depth of 9m and with summertime ground and ambient temperature assumption consistent with the UK seasonal values. This comparison is shown in Table 3.

Table 3

IEC60287	2D FEM (IEC Losses)	2D FEM (Benchmarked losses)
651A	670A	711A

A more detailed representation of the cable and the soil strata has resulted in a 9% increase on the rating that would be provided by IEC60287. To demonstrate the

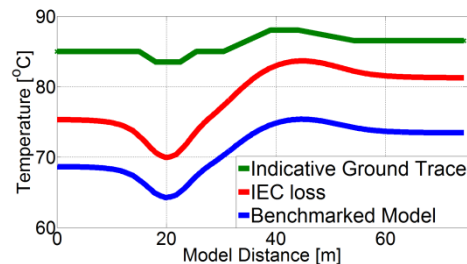
impact that a 3D representation of the landfall would have, a rating based on the design standard is compared against a 3D FEM with IEC losses and a 3D FEM with benchmarked losses. This comparison is shown in Table 4. Apart from representing the burial in 3D all parameters are consistent with the previously given ratings.

Table 4

IEC60287	3D FEM (IEC Losses)	3D FEM (Benchmarked losses)
651A	695A	735A

A more accurate representation of the cable burial and the cable has resulted in a 13% increase on the rating that would be provided by IEC60287. Figure 14 shows the modelled conductor temperature profiles along the length of the cable for IEC losses and losses in line with experimentation. It provides an explanation as to why a higher rating can be achieved.

Figure 14



Some longitudinal heat transfer occurs along the conductor, from the hot spot beneath the sea defence, towards the cooler locations (notably the drainage ditch). Additionally, some longitudinal heat transfer occurs through the soil region, particularly as the thermal resistance of most elements (other than the sea defence) is low. The contour of the sea defence and drainage ditch, increase the ground surface area per metre of cable (compared to the 2D assumption), meaning that additional heat can be extracted from the sea defence zone itself. This highlights the importance of using 3D models where cable routes meet such obstacles.

## 2.5 J-TUBE

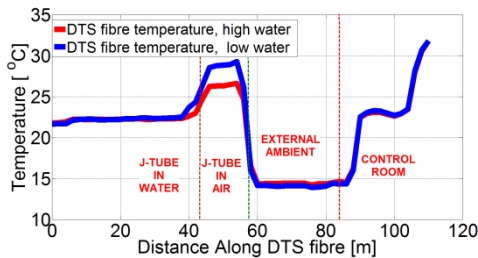
The J-tube (or any other cable protection system) may present a number of challenges to the rating of a cable. The

cable rises out of the sea enclosed within a cylinder that is typically made of steel. Heat is transferred between the cable and the environment through convection, conduction and radiation, with ambient conditions being seasonally variable. At present there are no internationally recognised design standards for the rating of cables in J-tubes. However, the methods described in [4] and [5] are commonly used.

To better understand the rating of a cable in a J-tube, a FEM was developed, validated against operational data and then the rating from the FEM compared with that obtained using common methods.

The initial model created was a 3D FEM with conductive heat transfer from the cable and J-Tube to the sea, convective and radiative heat transfer between the cable and the interior of the J-Tube and convective and radiative heat transfer between the exterior of the J-Tube and the environment. An example of the model output is shown in Figure 16. Initial modelling suggested that even with convective flow in the region between the cable and J-Tube there was little variation in temperature along the length of cable. This was supported by DTS measurement, see Figure 15. On this basis it was assumed that a 2D approximation of the J-Tube air region was reasonable.

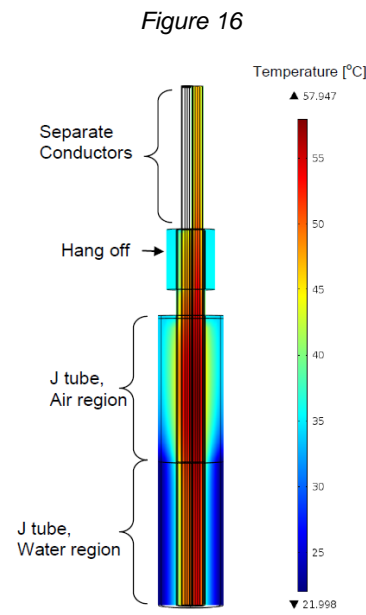
Figure 15



To compare the DTS results with the numerical model, a series of filler temperature probes need to be defined within the numerical model. The temperature probes are defined along a radial line out from the centre of the cable, in the middle between two conductors. The model was initially solved with full IEC losses and subsequently with the benchmarked losses. The summer ratings determined using the model and the methods described in [4] and [5] are summarised in Table 5 below. Assumptions regarding ambient



temperature, solar loading, J-Tube absorptivity and emissivity were consistent between each method for calculating the rating.



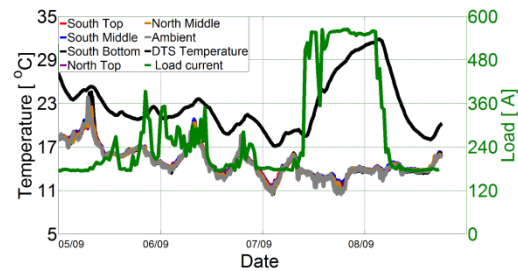
From Table 5 it is evident that the FE model increases the rating by 154A (or 27%) when compared with the Hartlein and Black model and 37A (5%) when compared against the ERA model. In all cases IEC losses are used.

Table 5

FE Model		Hartlein & Black	ERA	
IEC Losses	Benchmark losses	IEC Losses	IEC Losses	Benchmark losses
709A	735A	555A	672A	730A

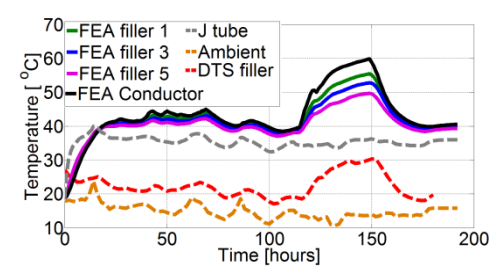
A J-Tube on an operational wind farm export cable route was instrumented to measure the temperature at different locations whilst subjected to varying cable current as is seen in service. The measured temperature profiles and the DTS data, from within the cable, are compared against the FE model developed. This was done as an initial attempt to validate the model. A sample of the recorded data is shown in Figure 17.

Figure 17



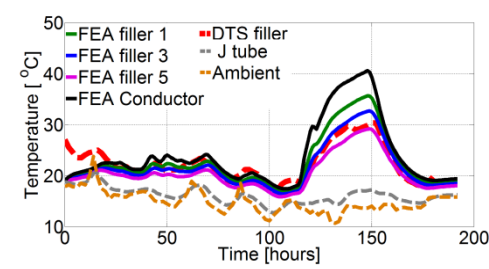
Measured load current and ambient temperature were used as time varying inputs to the FE model and model outputs for J-Tube cable interstices were compared to measurements. The benchmarked cable losses were used in this model. Figure 18 shows the comparison with an assumed solar flux of 1000Wm<sup>-2</sup>. It is clear from Figure 18 that the model is overestimating the temperature of both the J-Tube and the cable.

Figure 18



With the solar heat flux removed, Figure 19 shows that the numerical predictions give a better agreement with the experimental results during the period of the load step. There is less agreement between the model and measured data during the period of low load. This is suspected to be due to other ambient conditions, such as wind, which have not been accounted for within the model.

Figure 19



Overall the FE model shows reasonable agreement with the measured data that was

available. In order to further refine the model it would need to be compared over a longer period with measured data. Ideally the measured data would also include wind speed and solar radiation.

### 3 CONCLUSION

This paper highlights work undertaken to better understand the rating of export cables for offshore wind farms. This has been achieved by using experimentally obtained data to derive a detailed FE model of a cable, prior to implementing that cable model within regions along an export route that are potentially thermally limiting. In doing so, potential gains in the continuous rating of a cable were realised through a more accurate representation of the environment that the cable is in and the losses within a cable.

The levels of rating that seem attainable are unlikely to mean the difference between requiring an additional cable, or not, for a typical 500MW wind farm block. The rating increases are of a size that it could mean the cable cross section could be reduced with confidence. This would have a noticeable impact on the capital expenditure, in the order of £millions, associated with the cables. However, being able to use a lower number of cables would result in a more significant reduction, in the order of tens of £millions.

To attain more significant reductions in expenditure on cables, a fundamental shift in the way that cables were rated for offshore wind farms would be required. This approach would take advantage of the inherently variable nature of wind generation to achieve higher utilisation of the cable capacity. Doing so would require consensus on an approach that was acceptable to all stakeholders in terms of quantifying the risk of a continuous rating being exceeded. It would be necessary to design in suitable means of controlling wind farm output in order to mitigate that risk, meaning that the cable could no longer be considered as a passive component.

### 4 REFERENCES

- [1] IEC, "IEC 60287-1-1: Electric Cables - Calculation Of The Current Rating," International Electrotechnical Commission.
- [2] Anders G, Rating Of Electric Power Cables, IEEE Press Power Engineering Series, 1997.
- [3] Palmgren D, Karlstrand J, Hennings G "Armour Loss in Three Core Submarine XLPE Cables," in *International Conference on Insulated Power Cables*, 2011.
- [4] Coates M, "Rating Cables in J-Tubes," ERA Technology, 1988.
- [5] Hartlein RA and Black WZ, "Ampacity Of Electric Power Cables In Vertical Protective Risers," *IEEE transaction on power apparatus and systems*, vol. 102, no. 6, 1983.
- [6] Arnold AHM, "Eddy Current Losses in Multi-core Paper-Insulated Lead-Covered Cables, Armoured And Unarmoured, Carrying Balanced 3 Phase Current," *Journal of the Institution of Electrical Engineers, Part II - Power Engineering*, vol. 88, no. 1, pp. 52-63, 1941.